

## **Recent Status of the Experiments in the KSTAR Superconducting Tokamak Device**

**Yeong-Kook Oh, W.C. Kim, S.G. Lee, J.Y. Kim, W.H. Ko, S. H. Hahn, J. Kim, Y.M. Jeon,  
S.W. Yoon, W.W. Xiao, H.L. Yang, H.K. Kim, Y.S. Bae, K.R. Park, Y. Chu, J. G. Kwak,  
M. Kwon, and KSTAR Team**

National Fusion Research Institute (NFRI), Daejeon, Korea  
(ykoh@nfri.re.kr)

### **Abstract**

The KSTAR device has a mission to explore the scientific and engineering research under the high performance and steady-state plasma confinement, which are essential for the fusion reactor realization. KSTAR device has been operated in stable for four years since 2008. Major operation results in KSTAR were the first plasma achievement in 2008, shape control and H-mode achievement in 2010, and successful edge localized mode (ELM) suppression in 2011. The KSTAR device will be upgraded and operated to explore critical issues in steady-state confinement achievement and in preparing the ITER and fusion reactors.

### **1. Introduction**

The Korea Superconducting Tokamak Advanced Research (KSTAR) device has a mission to explore the scientific and engineering research under the high performance and steady-state plasma confinement, which are essential for the fusion reactor realization [1]. To contribute in world-wide fusion research and reactor engineering design, KSTAR has adopted the most outstanding research results from the present devices and will exploit high performance steady-state operation which will provide the core technology for ITER and future reactor designs. The key designed parameters of the KSTAR are compared with those of ITER in the Table 1. The basic designed operation parameters are toroidal field (TF) of 3.5 T, plasma current of 2 MA, pulse length up to 300 s. The plasma shape is capable of single null and double null with major radius of 1.8 m, minor radius of 0.5 m, elongation up to 2.0. The specific features in the KSTAR design are installation of the fully superconducting magnets, especially the first tokamak device adopting Nb<sub>3</sub>Sn superconductor for both TF and PF magnets [2]. The key engineering of the KSTAR device is similar to that of ITER as shown in Figure 1.

KSTAR device has been operated for four years since the construction and integrated commissioning of the tokamak device had been completed successfully. In 2008, the first plasma was successfully implemented in the level of 100 kA with circular cross section due to the limited hardware such as the PF magnet power supplies [3]. In 2009, plasma current was increased up to 500 kA by the stable plasma control system operation. In 2010, successful H-mode was achieved in KSTAR for the first time among the fully superconducting tokamak devices. To achieve the H-mode, there were major hardware upgrades such as installation of new in-vessel components and a new neutral beam in the range of 1.5 MW neutral beam injector (NBI) at 95 keV. In 2011, the H-mode has been sustained longer and the operational regime of plasma parameters has been significantly extended. Based on the achievement of high beta H-mode, as the main focus of the

campaign, various methods were applied for the edge localized mode (ELM) control by including resonant magnetic perturbation (RMP), supersonic molecular beam injection (SMBI), or vertical jogging and ECCD injection on the pedestal

In this paper, key features in terms of machine operation of superconducting tokamak and plasma commissioning will be reviewed. The stabilization of the plasma start-up, H-mode and ELM control in the superconducting tokamak will be introduced.

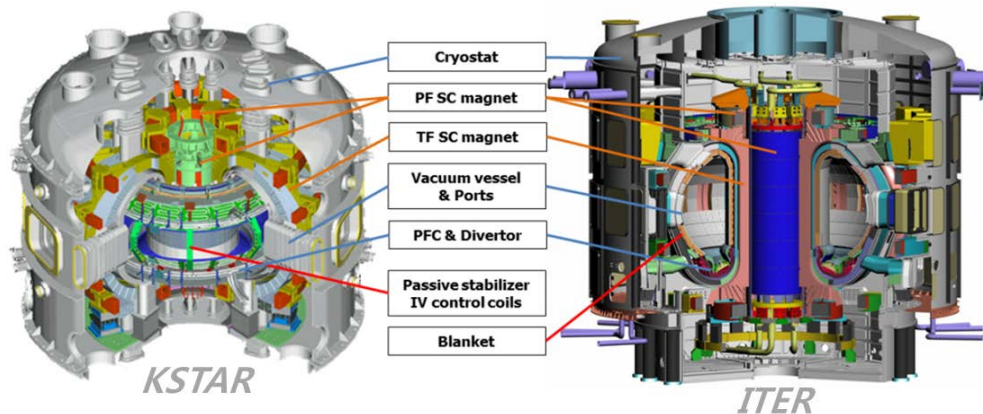


Figure 1. Schematic design comparison between KSTAR and ITER superconducting tokamaks.

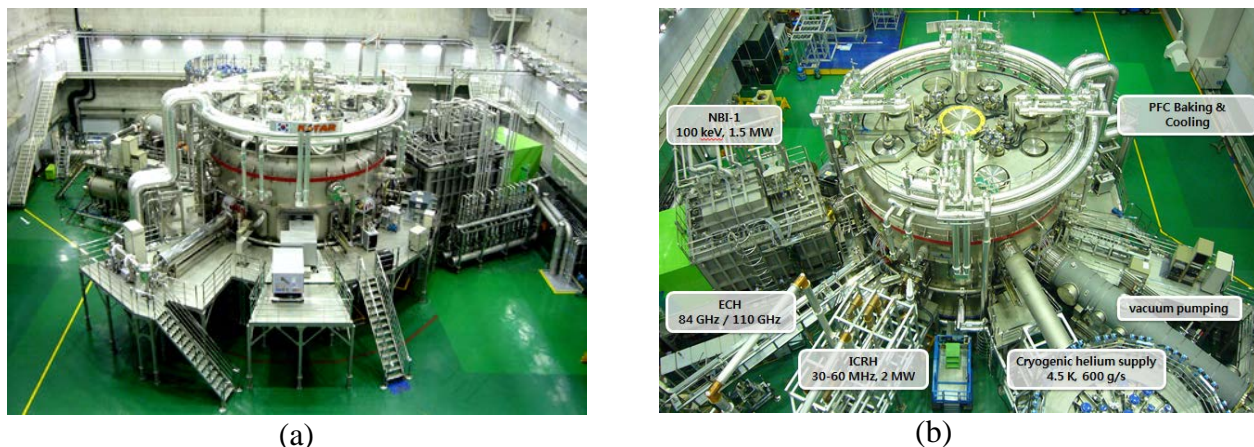


Figure 2. The status of KSTAR device with the ancillary heating and diagnostic systems before the plasma experiments, (a) viewed from the front and (b) from the top.

Table 1. Key design parameters of the KSTAR and ITER devices campaign.

KSTAR Parameters	KSTAR	ITER
Toroidal field, $B_0$ [T]	3.5	5.3
Plasma current, $I_p$ [MA]	2.0	15 (17)
Pulse length [s]	300	400
Normalized beta	5.0	1.8 (2.5)
Plasma shape	Double null, Single null	Single null
Major radius, $R_0$ [m]	1.8	6.2
Minor radius, $a$ [m]	0.5	2.0
Elongation, $\kappa$	2.0	1.7
Triangularity, $\delta$	0.8	0.33
Plasma volume [ $m^3$ ]	17.8	830
Plasma fuel	H, D	H, D, T
Superconductor	Nb <sub>3</sub> Sn, NbTi	Nb <sub>3</sub> Sn, NbTi
Auxiliary heating /CD [MW]	28	73 (110)

## 2. Engineering of the superconducting tokamak device

### 2.1 Vacuum and in-vessel components

The vacuum system in the KSTAR has two separate volumes. The primary vacuum is in the vacuum vessel for plasma discharge and the secondary vacuum is within the cryostat for thermal isolation of the superconducting magnets. The vacuum vessel has a volume of 100 m<sup>3</sup> is evacuated by using the pumping system with capacity of 42,400 l/s. Plasma facing components (PFCs), which consist of limiters, diverters, and passive stabilizers, were installed in the vacuum vessel as a plasma boundary [4]. All the PFCs are covered with graphite tiles as shown in Figure 3. Although the PFC system was designed to be actively water-cooled, they were passively cooled in 2010 and 2011 operations owing to the consideration of substantially low heat influx on the PFCs.

To reduce the impurity injection to the plasma, all of the PFCs baked up to maximum 260 °C using hot N<sub>2</sub> gas circulation, which was simultaneously performed with baking of the vacuum vessel up to 130 °C. In addition, D<sub>2</sub> and helium glow discharge cleaning (GDC) were performed before the plasma discharge. As a result, outgassing rate was decreased to  $7.80 \times 10^{-4}$  Pa·ℓ·s<sup>-1</sup> and the vacuum pressure reached below  $7.5 \times 10^{-6}$  Pa.

The segmented in-vessel control coils (IVCCs) which are composed of 12 segmented coils, four in the toroidal and three in the poloidal segments, were installed in vacuum vessel as shown in Figure 4(a) [4]. There are 8 conductors inside each coil and various coil combinations are capable by changing the electric connections as shown in Figure 4(b). The designed voltage and current rating of each coil is 900 V and 7.5 kA, respectively. The IVCC system is one of the unique features in KSTAR because it could provide wide physics experiments and flexibilities of plasma control through varying the formations of "picture-frame" coils for resonant magnetic perturbation (RMP), resistive wall mode (RWM), and field error correction (FEC) experiments. In 2010 the elongated plasma shape control was possible due to the fast vertical position control using the inner vertical

coils (IVC) operation. In 2011, ELM control experiments using RMP will be done with a toroidal mode number of 1 and 2. The IVCCs could be applicable for the plasma control to achieve steady-state confinement without ELM or disruption which is one of essential research topics in ITER and future fusion reactor.

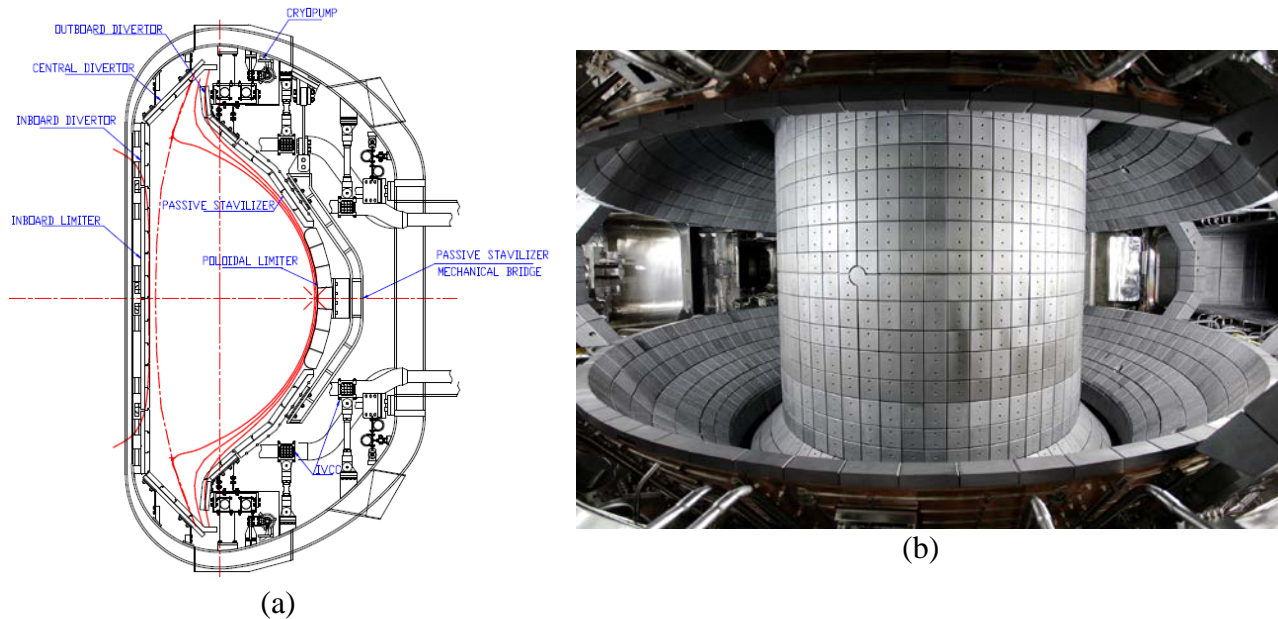


Figure 3. (a) The cross sectional drawing of the vacuum vessel and in-vessel components, and (b) bird eye view of the in-vessel components covered with graphite tiles in KSTAR.

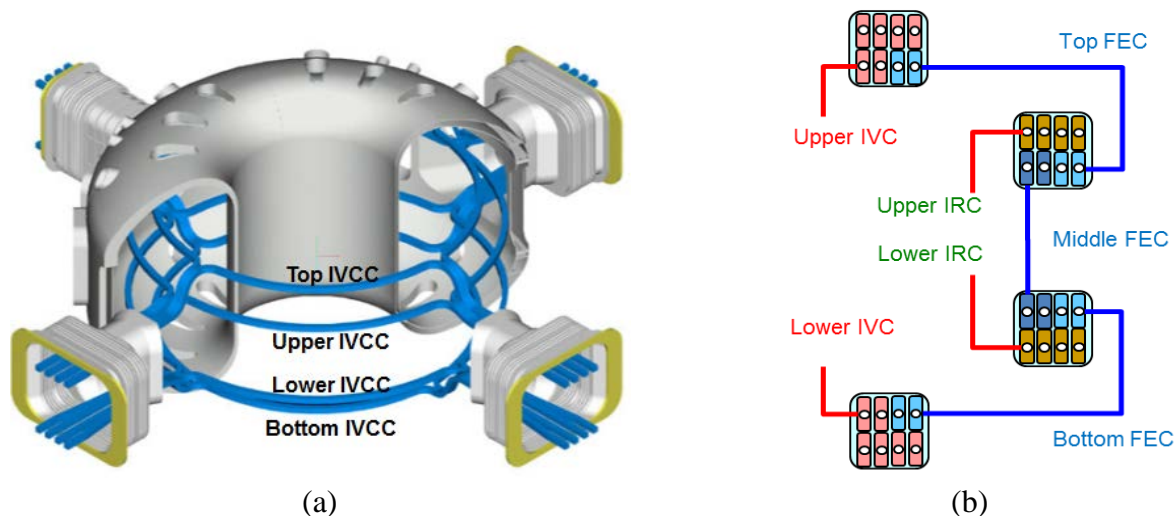


Figure 4. (a) The schematic configuration of the segmented in-vessel control coils, and (b) the electric connection between coils to generate 3 dimensional magnetic fields



## 2.2 Superconducting magnets

The magnet system of the KSTAR device consists of 16 toroidal field (TF) coils and 14 poloidal field (PF) coils as shown in Figure 5(a). One of major uniqueness of KSTAR is adopting the fully superconducting magnets, which are using the same Nb<sub>3</sub>Sn and NbTi conductor as ITER device [5]. It took about 20 days to cool down the KSTAR machine whose cold-mass is about 300 tons. After cool-down, the inspection of each coil was conducted such as leak from the magnet system, resistance change of the coil according to temperature, resistance of each terminal joints, high voltage insulation test.

The TF magnet was also charged up to designed value of 35 kA for more than 8 hours. The TF coil temperatures were stably maintained within deviation of 0.3 K. The maximum mechanical strain of the TF coil structure during charging up to 35 kA was about 680  $\mu\epsilon$  and it satisfied the operating criteria with 28% of 2,400  $\mu\epsilon$ . Mechanical strains of the TF coil structure is kept same range for the four operation campaign without any failure since 2008. The operation of the PF coils is controlled by the plasma control system (PCS). The designed current level of PF coils are about 25 kA for the plasma current of 2 MA. In 2011, the PF coils were operated in 15 kA due to the limited electricity. Single coil test has been conducted up to 25 kA for PF4L coil for the engineering verification. All the PF coils could be operated at designed current from 2013 after the installation of a motor generator system with 200 MVA electric power capacities. Normal operating sequence of the PF coils are (i) initial magnetization for the field null formation in vacuum vessel, (ii) blip for the plasma breakdown by the high inductive voltage, (iii) inductive current ramp by changing the flux, (iv) plasma shaping and position control, (v) ramp down after the plasma experiments. The non-linear magnetic field comes from the ferromagnetic material, Incoloy908, in the superconductor jacket was an obstacle in the plasma startup in 2008. After inclusion of the non-linear field effect in the startup scenario according to the field measurement, the reliable startup could be achieved.

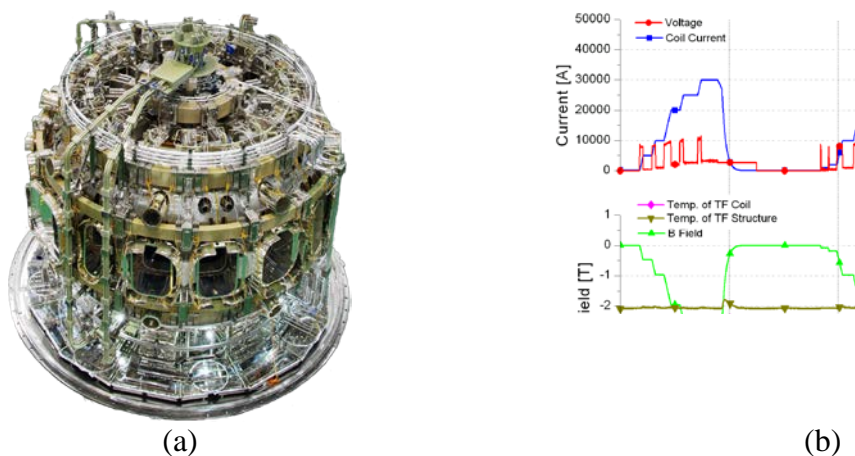


Figure 5. (a) The assembled superconducting magnet system, and (b) and the operation results of the TF magnet at 35 kA. It shows the stable operation with temperature variation within 0.3 K.

### 2.3 Heating and current drive systems

The KSTAR heating and current drive (H&CD) system contains the NBI, ICRF, LHCD, and ECH/ECCD systems [4]. The combination of multiple heating and current drive technologies is aimed at providing flexible control functions for current density and pressure profile in the KSTAR operation scenarios. The planned NBI systems are a D<sup>0</sup> neutral beam power of 12 MW at the beam energy of 100 keV with two beam lines and three ion sources in each beam line, a ICRF coupled heating power of 6 MW at 30~60 MHz, a LH heating power of 2 MW at 5 GHz, an EC heating power of 0.7 MW at 84 GHz and 110 GHz for start-up, and an EC heating power of 3 MW at 170 GHz for current drive and MHD mode stabilization, respectively.

Among the various H&CD systems described above, the available heating systems in 2012 experiments will be 3.5 MW neutral beam power for major plasma heating, ECH/ECCD systems with three kinds of frequencies. Two ECH systems with frequencies of 84 GHz and 110 GHz were used for the ECH-assisted plasma start up and a new 170 GHz ECH/CD system will be available for the off axis heating research. A 5 GHz, 0.5 MW, LHCD system will be installed for non-inductive current drive experiments in 2012 campaign.

One of the most important goals for the KSTAR tokamak is long pulse operation (300 s) to explore the physics of steady-state fusion plasmas. To support the steady state operation of KSTAR in near future, validation test of long pulse and high power neutral beam is required in advance of the upgrade of the second and third beam lines and next ion beam sources in the first KSTAR NBI system. Therefore, the 300-s long beam extraction was attempted for the first time in KSTAR with the beam energy of 80 keV. The pulse length is step by step increased, and finally the 300-s long pulse is successfully achieved. The beam current is 27 A, the arc power is 25 kW, and the beam perveance is 1.2  $\mu$ -P. The ion beam power is 2.16 MW, and the injected neutral beam power to the calorimeter is about 0.95 MW. Total beam energy to the calorimeter is 285 MJ. The long-pulse stable operation was possible owing to the very good control of the filament, arc discharge, acceleration, and deceleration power supplies. All the voltages of twelve filaments are constantly supplied by the voltage control mode in each local controller. The stable arc discharge is maintained by the constant arc power mode controlling gate of the IGBT switches. The constant gas pressure is also stably maintained using MFC in the neutralizer cell. The gas pressure in the ion source bucket chamber was not unfortunately measured.

In 2011, a new 170 GHz ECH/CD has been installed using ITER pre-prototype 170 GHz, 1 MW CW gyrotron developed by JAEA. The launcher for 170 GHz ECH/CD system is developed with capability of 1 MW and 5-10 s pulse duration in collaboration with PPPL and POSTECH. During 2011 KSTAR campaign, the maximum 600 kW with pulse duration of 10 s is achieved and injected to KSTAR plasma for the second and third harmonic condition.

## 2.4 Diagnostic system

Many advanced diagnostic systems as well as basic measurements have been developed in collaboration with domestic and international collaborators [6]. The layout of the diagnostic systems is shown in Figure 6. To study edge and pedestal physics, some diagnostics are dedicated for the profile measurements. Ion temperature profile and toroidal rotation profile were measured by X-ray imaging crystal spectrometers (XICS) and charge exchange spectroscopy (CES). Especially XICS showed the core rotation variation according to the operation mode and ECH heating. The ion temperature and toroidal velocity profile for H mode and L mode in KSTAR was measured by CES. In H mode condition, the pedestal structure was found in ion temperature and rotation speed as shown in Figure 7. The core rotation decrease under ECH heating was measured by CES and XICS.

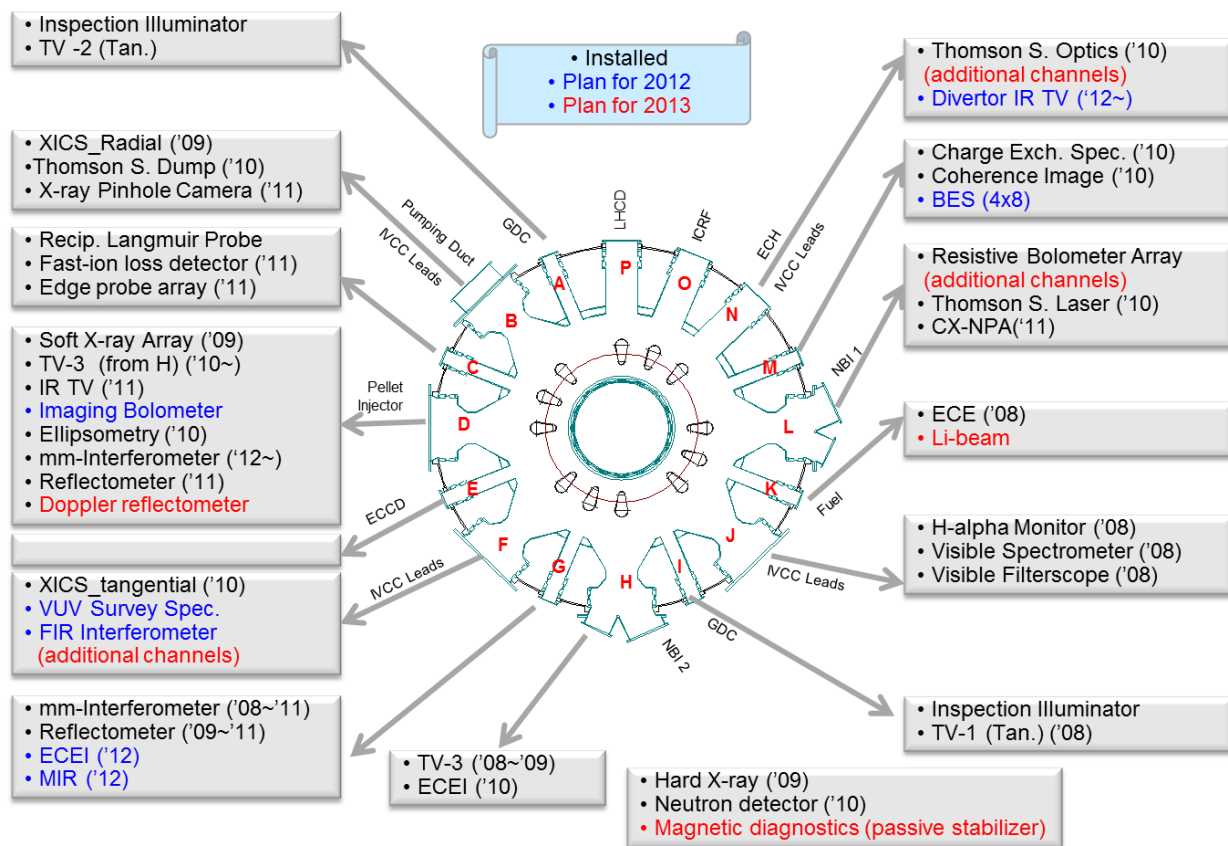


Figure 6. The layout and port allocation of the KSTAR diagnostic systems. The system installed already are colored in black, The system available at present are black colored, ones available in 2012 are in blue and the system planned to be installed in 2013 are in red.

For the electron temperature and density profile measurement, a Thomson scattering system has been installed and commissioned. The KSTAR Thomson scattering system has been installed and commissioned. The electron temperature and electron density profiles were measured during the

plasma shot. However most of signals included large level of noises from the electric power system and from the stray lights thus the evaluation of the electron temperature and density profiles was difficult. More reliable measurement is expected in 2012 because the laser system will be upgraded with a 5J, 100Hz Nd:YAG Laser system which was developed by JAEA for ITER Thomson system.

Beam emission spectroscopy (BES) can measure electron density from light intensity of Doppler-shifted line emission of neutral beam and its fast measurement speed up to several MHz enables fluctuation study on electron density. A BES system based on direct imaging avalanche photo diode (APD) camera has been designed. A trial system has been installed for evaluating feasibility of the design. Test of the trial BES system was performed during several H-mode control experiments and some interesting data could be gathered. In 2012 campaign, small part of beam will be delivered to a slow camera for simultaneous measurements of density profile with fast APD camera for density fluctuation measurements. This feature enables relative density measurements via calibrations between detectors. These relative profiles can be converted to absolute values by comparison with other density diagnostics such as a Thomson scattering or an interferometry. In 2013 campaign, a Li-beam injection system will be installed for the BES system. This makes the density profile measurement available on the edge region with  $\sim 10\mu\text{s}$  independent with the operation of heating beam.

The filamentary nature and dynamics of ELMs in high-confinement mode plasmas have been visualized in 2D via electron cyclotron emission imaging (ECEI). The ELM filaments rotating with a net poloidal velocity are observed to evolve in three distinctive stages. An additional ECEI system will be installed in 2012 for the 3D interpretation of the filamentary dynamics.

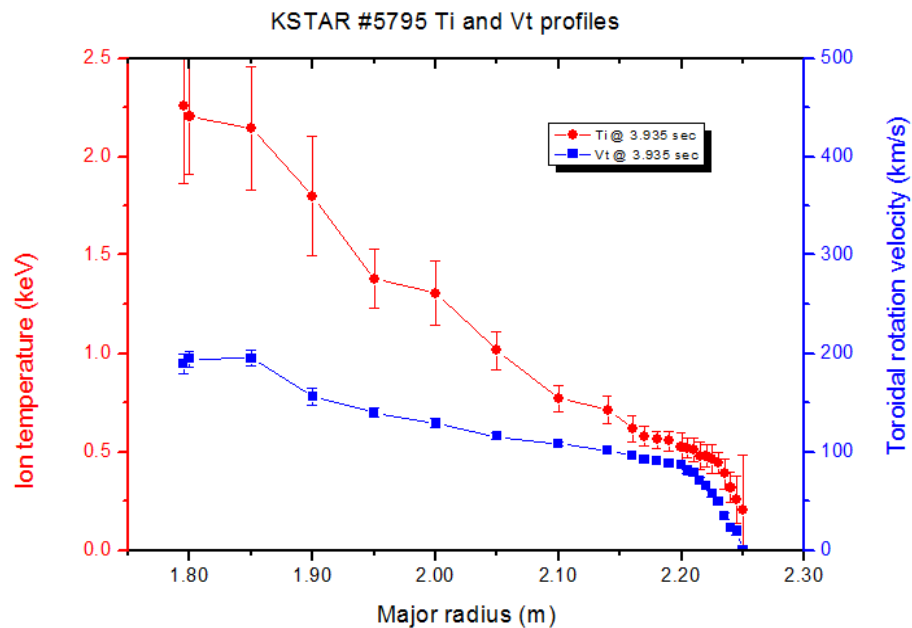


Figure 7. The ion temperature and toroidal rotation profile measured by CES in H-mode condition. The pedestal structure could be seen in both ion temperature and velocity profiles.



### 3. Plasma experiments and analysis

#### 3.1 Plasma start-up and shape control

The plasma current and shape in KSTAR is controlled by a plasma control system (PCS), which is using Linux cluster with 8 processes, and has control frequency up to 20 kHz. The plasma start-up scenario was modified to cancel out the effect of ferromagnetic material in the superconducting coils. The developed scenario from 2010 by the time-series analysis of static nonlinear calculations has several improvements as compared with the previous start-up scenarios used in the 2008 and 2009 KSTAR campaigns [7]. The achieved plasma current level was increased every year as shown in Figure 8. In 2008, the first plasma target was achieved with over 100 kA. The plasma control in current level, shaping, and position in 2010 and 1 MA was achieved.

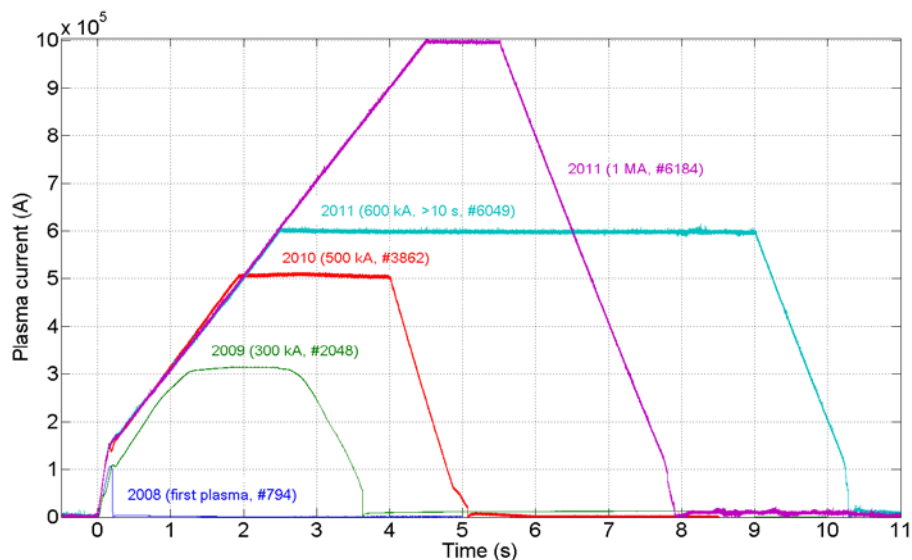


Figure 8. Progress of the plasma current in KSTAR. First plasma in the level of 100 kA was achieved in 2008 and 1 MA range of current was achieved in 2011. The designed level of plasma current in KSTAR is 2 MA for 300 s.

The plasma confinement is usually improved when the shape of plasma is elongated and shaped compared to circular cross section. However the elongated plasma tends to be unstable in the vertical position. The plasma facing components was installed according to the optimum plasma shape. Initial shape control is done by feed-forward by adjusting the control parameters. An advanced shape control was implemented based on the real-time EFIT (rtEFIT) and Isoflux algorithm for the reliable shape control and long pulse sustainment in 2011. Two different algorithms are applied for the design of a plasma discharge. The “isoelong” algorithm is designed for  $I_p$  rampup/down, controlling a limited plasma shape transitioning into a diverted shape and vice versa. The “isodnull” is intended to maintain a double-null diverted shape, defining the reference flux as the flux at either of X-point. In KSTAR, the flux at the lower X-point was chosen to the reference. As shown in Figure 9, isoflux control based on the real-time EFIT started at 1.5 s, and

the change to isodnull happens after both the diverted field structure and the  $I_p$  plateau are obtained by the isoelong algorithm.

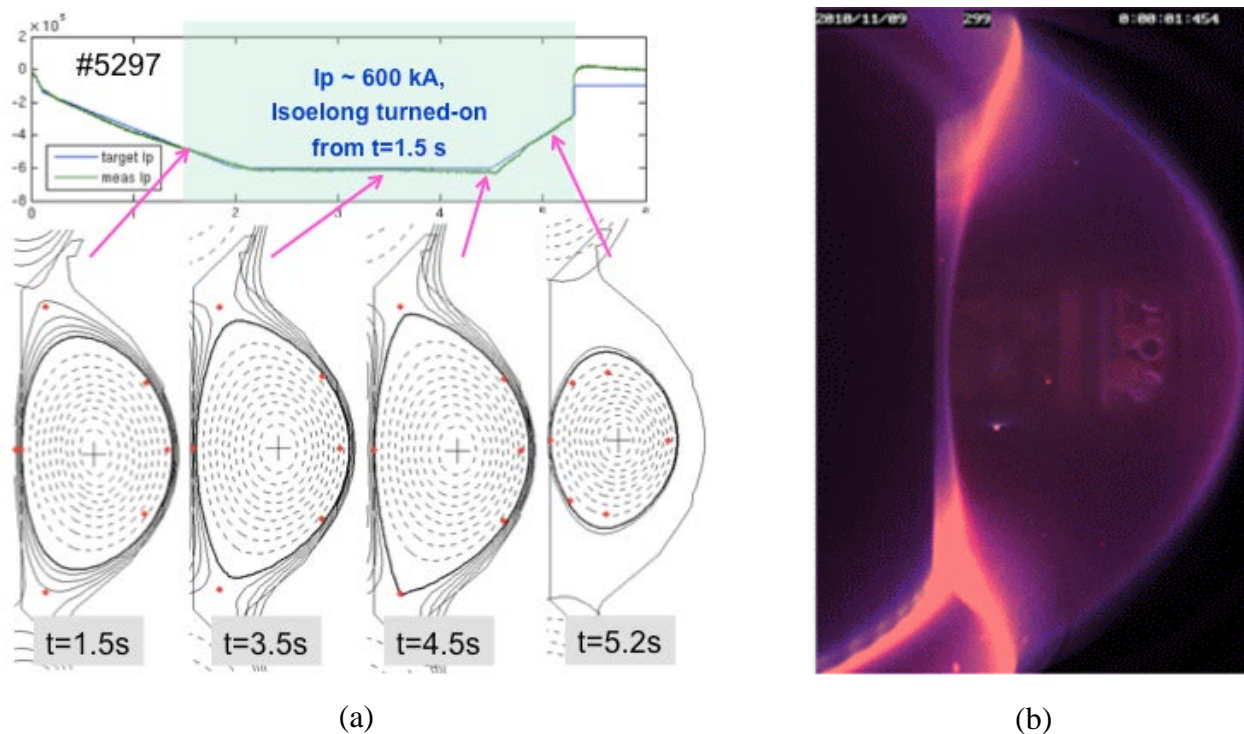


Figure 9. (a) Typical iso-flux control of plasma during current ramp up, flattop, and ramp-down phase, and (b) the image of shaped plasma discharge. Plasma was detached from the plasma facing components except upper and lower divertors.

### 3.2 H-mode confinement and ELM characteristics

The transition from a standard confinement mode (L-mode) to an improved confinement regime (H-mode), the so-called L–H transition, has been observed in KSTAR from 2010 experiments. It has been found that an L–H transition requires a minimum threshold power ( $P_{thr}$ ), which is affected by multiple factors such as toroidal magnetic field ( $B_T$ ) and the direction of ion grad-B drift to the X-point, the plasma shape and surface area ( $S_{surf}$ ), the wall condition, the ion species, and the electron density ( $n_e$ ). In KSTAR, typical edge localized mode (ELMy) H-mode discharges have been obtained with the combined auxiliary heating of NBI and ECRH [8]. After the transition to H-mode, stored energy was increased by the enhanced confinement and large number ELM spikes occurred in D $\alpha$  signal as shown in Figure 10(a). The minimum external heating power required for the L–H transition is about 0.9MW for a line-averaged density of  $\sim 2.0 \times 10^{19} \text{ m}^{-3}$  as shown in Figure 10(b).

KSTAR H-mode plasmas exhibit three distinctive types of ELMs; 1) large type-I ELMs with low ELM frequency ( $f_{ELM}=10\text{-}50\text{Hz}$ ) and good confinement ( $H_{98(y,2)}=0.9\text{-}1$ ), 2) smaller, possibly type-III, ELMs with high ELM frequency ( $f_{ELM}=50\text{-}250\text{Hz}$ ) and poorer confinement ( $H_{98(y,2)}=0.7\text{-}0.8$ ), and 3)

a mixed, large and small, ELM regime with good confinement ( $H_{98(y,2)} \sim 1$ ). The NBI power scan showed that ELM frequency increased with increasing input power for large ELMs, which is a typical behavior of type-I ELMs. The apparent ELM type changes with different plasma conditions and even during a single discharge. For example, high electron density seems to lead to the small ELMy H-mode regime.

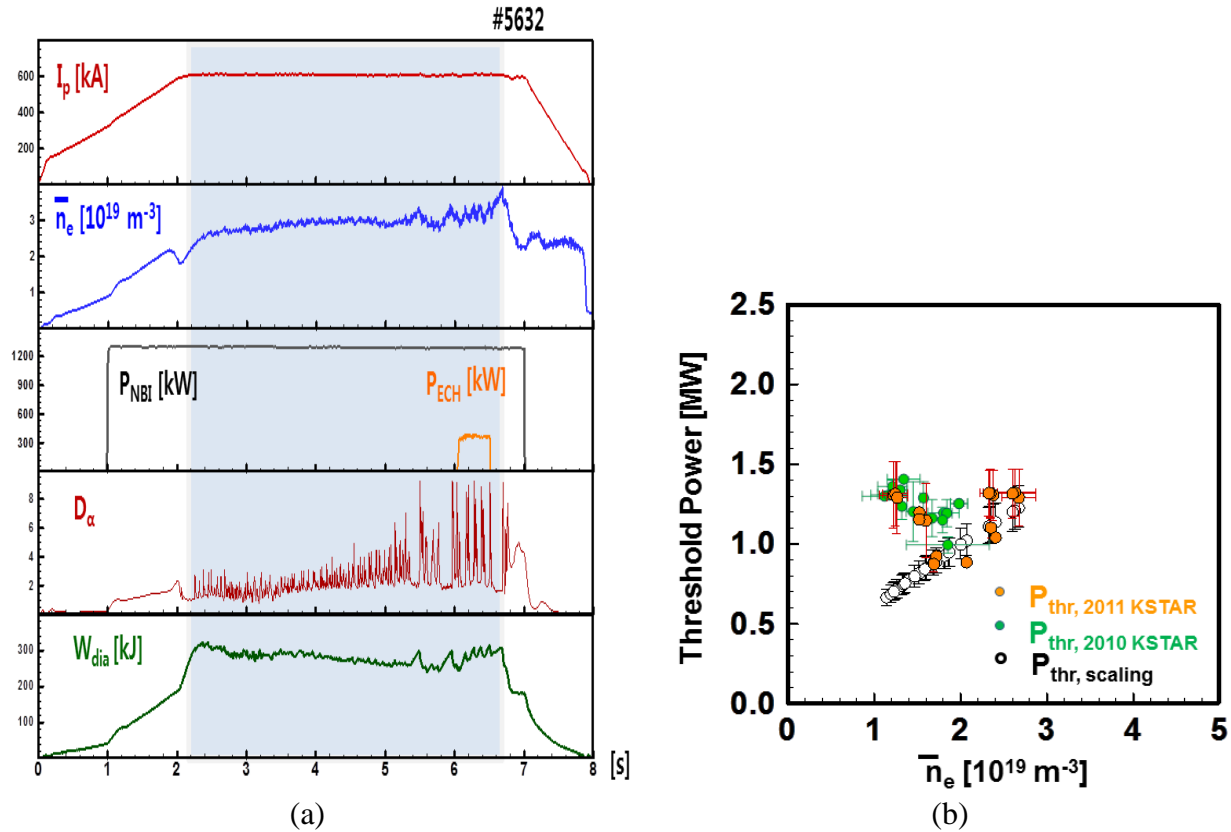


Figure 10. (a) The typical H-mode transition (shot 5632) the stored energy is increased and large amount ELM signal spikes were observed, and (b) existence of minimum power threshold for L-H transition at  $n_e \sim 2 \times 10^{19} \text{ m}^{-3}$ .

### 3.3 ELM control experiments in H-mode operation

The intermittent and transient power load onto the plasma facing components induced by large type-I ELMs in high-performance H-mode plasmas is one of the critical issues for the mechanical integrity and lifetime of PFCs in future high-power H-mode devices, such as the International Thermonuclear Experimental Reactor (ITER). In this regard, several methods to control ELM stability have been investigated in KSTAR including (i) external non-axisymmetric magnetic field, (ii) sonic molecular beam injection (SMBI), (iii) vertical jogging and (iv) local edge heating by electron cyclotron heating [9].

The ELM was successfully suppressed in KSTAR by applying small amount of non-axisymmetric MPs [10]. ELM-suppression by RMP has been first reported in DIII-D by applying  $n=3$  RMP and

has not been reproduced in other devices so far. Particularly this achievement can be highlighted by a point that ELM-suppression was achieved by applying  $n=1$  RMP instead of  $n=3$  RMP, suggesting wider potential of ELM control by MPs. As described in section 2.1 and shown in Figure 11 (a), RMP coils are installed in vacuum vessel just behind the plasma facing components and are segmented in 12 picture frame shaped coils. The time evolution of ELM-suppressed RMP discharge (red) in comparison with a reference ELMy H-mode discharge (black) is shown in Figure 11(b). From the  $D_\alpha$  signal, it can be clearly seen that the ELMs were initially intensified when the  $n=1$  MP was applied and then suddenly disappeared (suppressed) from 3.5 s. In the initial intensified ELM phase, the line-averaged electron density ( $\langle n_e \rangle$ ), the total stored energy ( $w_{tot}$ ), and the toroidal rotation ( $V_{tor}$ ) decreased by a  $\sim 10\%$ , whereas the central  $T_e$  and  $T_i$  didn't change much. However, in the ELM suppressed phase, most of parameters got stationary except the gradual increase of line-average density. The control tendency of ELM was changed according to the changing of the modes and phase angles. Most effective condition for ELM suppression was  $n=1$  at  $+90$  phase angle. The additional ELM suppression investigation for  $n=1$  and  $m=2$  modes by increasing the current level in RMP power supplies.

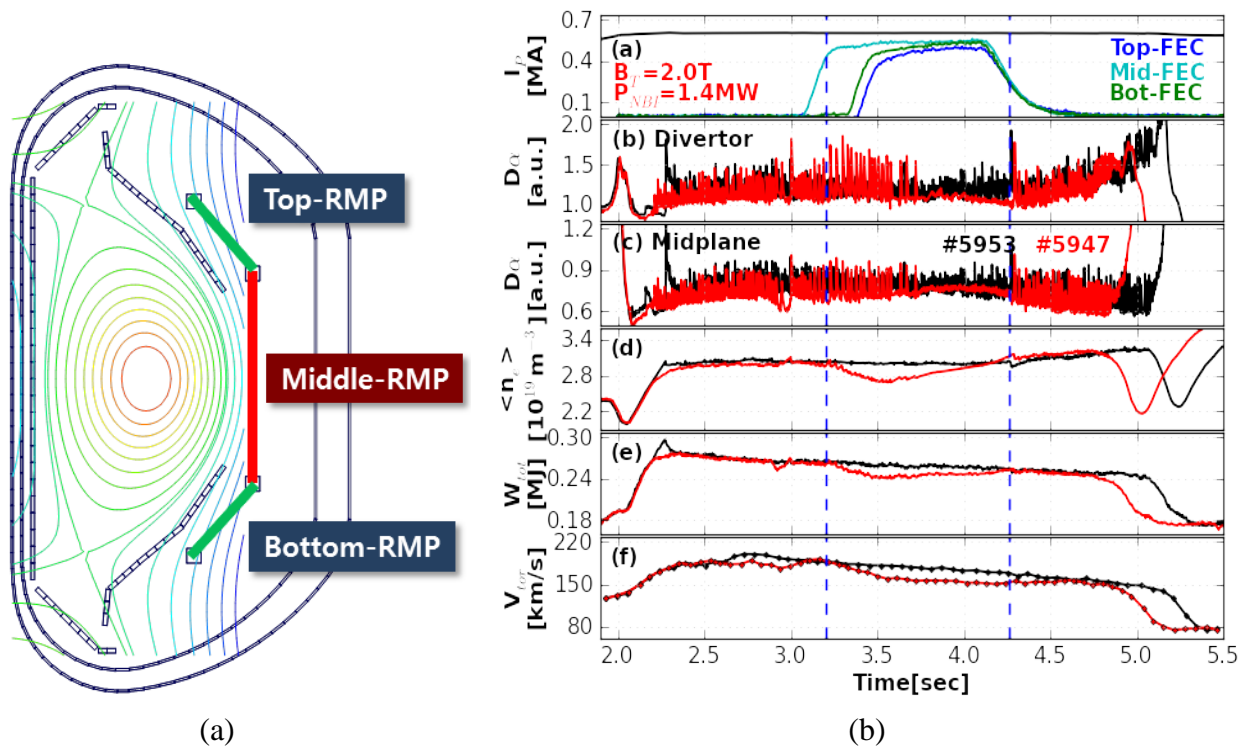


Figure 11. (a) The location of the segmented in-vessel RMP coils, and (b) a representative ELM suppressed RMP discharge in comparison with a reference ELMy H-mode discharge.

By injection of the SMBI at the gas pressure  $\sim 1$  MPa into the H-mode pedestal region, the characteristic of ELM has been changed. The experimental results showed that the frequency of ELM was increased from about 40 Hz to about 98 Hz and amplitude was decreased for a finite duration period after SMBI [11]. The parameters of discharge are plasma current of 0.6 MA, toroidal field of 2.0 T and line average density of  $3.4 \times 10^{19} m^{-3}$ . Total heating power (ECRH and

NBI) is about 1.7MW. The line average density was increased about 9% after one SMBI pulse injection. The global confinement was not destroyed by SMBI while a small drop of the store energy after the SMBI pulse injection.

In order to apply fast vertical jogs from a plasma equilibrium position, a sawteeth-shaped waveform was programmed in the vertical position reference of plasma control system. The axisymmetric part of the IVCC produced an appropriate radial field which was superposed with the equilibrium field according to the PCS command. The experiment aimed to lock the ELM frequency to the frequency of vertical jogs by varying the amplitude, velocity, and frequency of vertical jogs. By doing this, basic characteristics of vertical jogs was studied such as the ELM trigger timing in KSTAR discharges. When the excursion amplitude was increased in order to oscillate the equilibrium between lower single null (LSN) and upper single null (USN) configurations, multiple ELM triggering phenomena occurred. The first ELM was triggered when the plasma reached its lowest position. The second and third ELMs happened near the maximum upward speed as already observed in the moderate excursion case. Furthermore, ELMs were triggered only around the LSN configuration although the plasma periodically oscillated between LSN and USN configurations with a very similar excursion level and speed.

There is also possibility of ELM control by direct heating or current drive in the pedestal region which will influence the peeling ballooning stability boundary of the ELM. The main heating schemes are ECH, ECCD, and lower hybrid current drive (LHCD) for the local heating and/or current drive in the narrow width of the pedestal which is typically a few centimeters in the KSTAR discharges. In the 2011 KSTAR campaign, the initial experiments of pedestal ECH/ECCD have been done by using both 170 GHz and 110 GHz ECH systems. The maximum available EC power available is 0.3 MW for 110 GHz and 0.6 MW for 170 GHz, respectively. Setting up the toroidal field at plasma center as  $B_{T0} = 2.3$  T and tilting the mirrors toroidally and poloidally targeting the upper region above the midplane. It is possible to deposit EC power both at the inboard and the outboard pedestal regions simultaneously near the position of the pedestal top thus maximizing pedestal heat deposition. In this case, the power from the 110 GHz gyrotron could be deposited at the upper outer region and the power from the 170 GHz gyrotron could be deposited at upper inboard side around. In KSTAR discharge #6313, after the L-H transition, ECH was injected for the period  $t=2.6-3.1$  s. The ELM frequency increased from about 25 Hz to about 40 Hz during the ECH injection as shown the  $D\alpha$  trace. In addition, the line-averaged electron density decreased and the global toroidal rotation also decreased. However, the stored energy did not change significantly. This may be due to the additional power from ECH in the pedestal. In the next campaign, the effect of ECCD will be further investigated by optimizing the ECCD efficiency.

#### **4. Summary and future plan**

The KSTAR is aimed at advanced tokamak (AT) research and it has unique features in the machine engineering and operation in terms of superconducting machine and AT research. Key components of the KSTAR has been constructed and operated stable for four years since the first plasma operation. One of the unique features of KSTAR is segmented 3D non-axisymmetric picture frame coils in vacuum vessel for the fast feedback control of plasma position and stability control. By



using the control coils the H-mode plasma confinement and successful ELM mitigation was possible in 2011 campaign. The TF magnet was operated up to 35 kA in stable for several hours with temperature rising within 0.3 K. The successful construction and operation experience of the Nb<sub>3</sub>Sn superconducting magnets in KSTAR could be a strong benchmark for the ITER magnet system development. The plasma start up scenario was optimized by compensating the field distortion from the ferromagnetic material in the superconducting coil. The plasma current reached up to 1 MA and shape control with elongation up to 1.9 by the operation of the vertical control coils. The ELMy H-mode was successfully produced at a plasma current of 0.6 MA. The control of ELM was studied as a high priority research topic for ITER. The ELM mitigation and suppression was successfully achieved by using the RMP coils at n=1 configuration, supersonic molecular beam injection, vertical jogging and ECH injection.

KSTAR will be operated and continuously upgraded in performance to achieve the research goals of exploring the high performance steady-state confinement which are essential for ITER and future fusion reactors [12]. The long term operation plan is classified into four operation stages. In the first stage of five years from 2008 to 2012, the major goal is to get stable plasma confinement to reach the basic plasma performance which is compatible with that of other present tokamaks. In the second phase, the major goals are to achieving the long pulse H-mode confinement and to explore the controllability of the ELM, disruption, H/L mode, and profile in the superconducting tokamak. The system will be upgraded to meet the experimental goals such as heating system upgrade in the range of 10 MW and long pulse capability, diagnostic systems for profile measurement and 2D/3D visualization, and plasma pacing components replacement with tungsten material. From the third phase the operation and experiments will be targeted for the research essential for high performance reactor operation such as stable operation under the high beta, high non-inductive bootstrap current condition and solving the relevant engineering issues.

## 5. Acknowledgement

The authors appreciate the strong collaboration on the KSTAR experiments from the Korean domestic and international institutions. The remarkable contributions from the domestic collaborators in KSTAR experiments are as follows; the development of 2D ECE imaging diagnostic system by POSTECH, the neutral beam system development by KAERI, Soft x-ray diagnostic system development by KAIST, edge probe diagnostic system by Hanyang Univ., and theoretical analysis by SNU and WCI.

The outstanding contributions from the international collaborators are as follows; DIII-D team in General Atomics contributed the stable plasma startup and control by developing the KSTAR plasma control system, and PPPL team has developed the ECH launcher system and joined in 3-D field experiments. ORNL has developed the filterscope diagnostic system and participated at the H-mode experiments. Columbia U. also attended the MHD experiments. NIFS in Japan has developed several key diagnostic systems including resistive Bolometer, imaging bolometer, ECE radiometer, and Polychrometer for Thomson scattering. JAEA has collaborated in heating system development including a 170 GHz ECH/CD gyrotron, and participated at plasma experiments including ECH wall conditioning. ASIPP in China has developed the multi-channel integrator

system for magnetic diagnostic and SWIP has collaborated in the SMBI experiments. Wigner RCP in Hungary has collaborated in BES diagnostic and ANU in Australia in MSE diagnostics.

This work was supported by the Korean Ministry of Education, Science and Technology under the KSTAR project.

## 6. References

- [1] G.S. Lee, et al., “Design and construction of the KSTAR tokamak”, Nuclear Fusion, Vol. 41 (2001) pp. 1515-1523.
- [2] Y.K. Oh, et al., “Completion of the KSTAR construction and its role as ITER pilot device”, Fusion Engineering and Design, Vol. 83 (2008) pp. 804-808
- [3] Y.K. Oh, et al., “Commissioning and initial operation of KSTAR superconducting tokamak”, Fusion Engineering and Design, Vol. 84 (2009) pp. 344-350
- [4] H.L. Yang, et al., “Development of KSTAR in-vessel components and heating systems”, Fusion Engineering and Design, Vol. 86 (2011) pp. 588-592.
- [5] Y.K. Oh, et al., “Superconductor application to the magnetic fusion devices for the steady-state plasma confinement achievement”, *submitted to the* Superconductors – properties, technologies, and applications. (ISBN 979-953-307-233-2).
- [6] J.H. Lee, et al., “Diagnostics for first plasma and development plan on KSTAR”, Review of Scientific Instruments, Vol. 81 (2010) p. 063502.
- [7] J. Kim, et al., “Stable plasma start-up in the KSTAR device under various discharge conditions”, Nuclear Fusion, Vol. 51 (2011) p. 083034.
- [8] S.W. Yoon, et al., “Characteristics of the first H-mode discharge in KSTAR”, Nuclear Fusion, Vol. 51 (2011) p. 113009.
- [9] J. Kim, et al., “ELM Control Experiments in the KSTAR Device”, *submitted to the* Nuclear Fusion.
- [10] Y.M. Jeon, et al., "Suppression of Edge Localized Modes in High-Confinement KSTAR Plasmas by Non-Axisymmetric Magnetic Perturbations", *submitted to the* Physics Review Letter.
- [11] W.W. Xiao, et al., “ First Signatures of ELM Mitigation by Supersonic Molecular Beam Injection in KSTAR” *submitted to the* Physics Review Letter.
- [12] J.G. Kwak, et al., “Key features in the operation of KSTAR”, submitted to 2011 IEEE/NPSS 24<sup>th</sup> Symposium on Fusion Engineering, (2011) SO1B-2.